The Acid-Mediated Denaturation Pathway of Transthyretin Yields a Conformational Intermediate That Can Self-Assemble into Amyloid†

Zhihong Lai, Wilfredo Colón,‡ and Jeffery W. Kelly*

Department of Chemistry, Texas A&M University, College Station, Texas 77843-3255

Received October 20, 1995; Revised Manuscript Received March 15, 1996⊗

ABSTRACT: Transthyretin (TTR) amyloid fibril formation is observed during partial acid denaturation and while refolding acid-denatured TTR, implying that amyloid fibril formation results from the self-assembly of a conformational intermediate. The acid denaturation pathway of TTR has been studied in detail herein employing a variety of biophysical methods to characterize the intermediate(s) capable of amyloid fibril formation. At physiological concentrations, tetrameric TTR remains associated from pH 7 to pH 5 and is incapable of amyloid fibril formation. Tetrameric TTR dissociates to a monomer in a process that is dependent on both pH and protein concentration below pH 5. The extent of amyloid fibril formation correlates with the concentration of the TTR monomer having an altered, but defined, tertiary structure over the pH range of 5.0−3.9. The inherent Trp fluorescence-monitored denaturation curve of TTR exhibits a plateau over the pH range where amyloid fibril formation is observed (albeit at a higher concentration), implying that a steady-state concentration of the amyloidogenic intermediate with an altered tertiary structure is being detected. Interestingly, 1-anilino-8-naphthalenesulfonate fluorescence is at a minimum at the pH associated with maximal amyloid fibril formation (pH 4.4), implying that the amyloidogenic intermediate does not have a high extent of hydrophobic surface area exposed, consistent with a defined tertiary structure. Transthyretin has two Trp residues in its primary structure, Trp-41 and Trp-79, which are conveniently located far apart in the tertiary structure of TTR. Replacement of each Trp with Phe affords two single Trp containing variants which were used to probe local pH-dependent tertiary structural changes proximal to these chromophores. The pH-dependent fluorescence behavior of the Trp-79-Phe mutant strongly suggests that Trp-41 is located near the site of the tertiary structural rearrangement that occurs in the formation of the monomeric amyloidogenic intermediate, likely involving the C-strand−loop−D-strand region. Upon further acidification of TTR (below pH 4.4), the structurally defined monomeric amyloidogenic intermediate begins to adopt alternative conformations that are not amyloidogenic, ultimately forming an A-state conformation below pH 3 which is also not amyloidogenic. In summary, analytical equilibrium ultracentrifugation, SDS−PAGE, far- and near-UV CD, fluorescence, and light scattering studies suggest that the amyloidogenic intermediate is a monomeric predominantly β-sheet structure having a well-defined tertiary structure.

Transthyretin (TTR),[1] also known as thyroxin binding prealbumin, is found in human plasma (0.2−0.3 mg/mL) as a tetramer of identical 127 residue subunits, each containing 1 cysteine residue which does not participate in disulfide formation. The X-ray crystal structure shows that each TTR subunit adopts a predominantly β-sheet structure, best described as a β-sheet sandwich where one four-stranded β-sheet interacts in a face-to-face fashion with another four-stranded β-sheet, forming the hydrophobic core of the protein (Blake et al., 1974, 1978; Hamilton et al., 1993). The remainder of the structure is predominantly loops and turns with only one short α-helix in the loop connecting strands E and F. The monomers dimerize through an intermolecular antiparallel β-sheet interaction involving two H strands yielding an eight-stranded β-sandwich (Figure 1). The two dimers interact to form a tetramer through hydrophobic interactions involving the loop regions adjoining β-strands G and H and β-strands A and B.

Transthyretin binds to the nonpeptidic hormone thyroxin in a central channel which runs through the tetramer (Nilsson et al., 1975; Blake & Oatley 1977; Wojtczak et al., 1992). Tetrameric transthyretin also typically binds to 1 mol of retinol binding protein (RBP), which in turn binds to vitamin A and prevents the 21 kDa RBP−vitamin A complex from being removed from the plasma by glomular filtration in the kidneys (Raz & Goodman, 1969; Jaarsveld et al., 1973; Monaco et al., 1995). TTR, like other amyloidogenic proteins, is turned over rapidly in plasma ($t_{1/2}$ is about 1.5−2.5 days), possibly by a receptor-mediated process (Makover et al., 1988; Divino & Schussler, 1990). In certain individuals transthyretin is converted into an insoluble, highly associated fibrillar quaternary structure called amyloid, which appears to cause familial amyloid polyneuropathy (FAP) and senile systemic amyloidosis (SSA) either through its neu-

† We gratefully acknowledge the financial support of the National Institutes of Health (R29 DK46335-01), the Searle Scholars Program/The Chicago Community Trust, and the Alzheimer's Association/Vivian L. Smith Foundation Pilot Research Grant.

* To whom correspondence should be addressed.

‡ Present address: Institute for Cancer Research, Fox Chase Cancer Center, Philadelphia, PA 19111.

⊗ Abstract published in *Advance ACS Abstracts,* May 1, 1996.

[1] Abbreviations: TTR, transthyretin; FAP, familial amyloid polyneuropathy; SSA, senile systemic amyloidosis; Z 3-14, *N*-tetradecyl-*N,N*-dimethyl-3-ammonio-1-propanesulfonate; ANS, 1-anilino-8-naphthalenesulfonic acid; SDS−PAGE, sodium dodecyl sulfate−polyacrylamide gel electrophoresis; CD, circular dichroism; OD, optical density.

S0006-2960(95)02501-3 CCC: $12.00

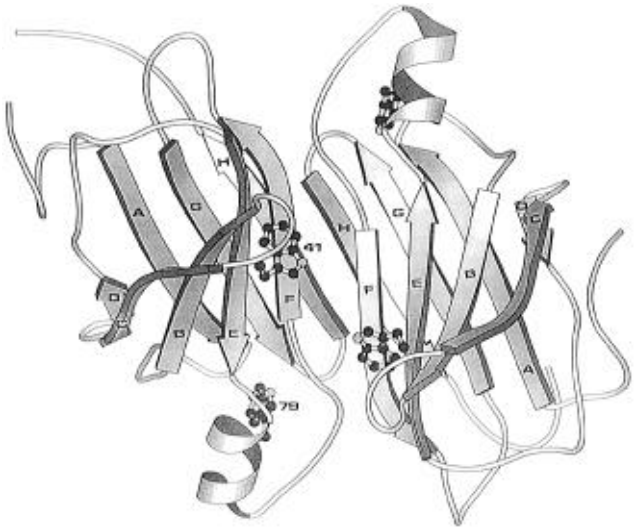

FIGURE 1: Ribbon diagram of the TTR dimer explicitly showing the indole side chains of the Trp residues. The AB-loops projecting from the back face in this view facilitate interactions with another dimer, leading to tetrameric TTR having a central channel at the dimer−dimer interface (Blake et al., 1978).

rotoxicity and/or by physically interfering with normal organ function (Benson, 1989; Benson & Wallace, 1989; Furuya et al., 1991; Jacobson & Buxbaum, 1991). While the main component of amyloid fibrils in SSA is wild-type TTR and fragments thereof, 1 of over 40 different TTR variants is found to predominate in the amyloid deposits of FAP patients (Saraiva et al., 1983, 1984, 1988; Cornwell et al., 1988; Westermark et al., 1990; Benson, 1989; Benson & Wallace, 1989; Stone, 1990; Saraiva, 1995). SSA affects 25% of the population over 80 years of age, while FAP affects only 1 in 10^5-10^6 individuals. In FAP patients, full-length variant transthyretin is usually the predominant fibril component (Benson, 1989). The single site mutations that cause FAP onset in the second to third decade of life do not significantly change the tertiary or quaternary structure of tetrameric TTR; instead they appear to function by destabilizing the TTR tetramer in favor of the amyloidogenic intermediate, which self-assembles into amyloid fibrils under mildly denaturing conditions (McCutchen et al., 1993, 1995; Steinrauf et al., 1993; Hamilton et al., 1993; Terry et al., 1993).

Amyloid fibrils, regardless of clinical syndrome, are insoluble deposits of otherwise soluble protein or protein fragments which self-assemble into fibrils of ≈100 Å in diameter and of variable length as discerned by electron microscopy (Cohen & Calkins, 1959; Eanes & Glenner, 1968; Pras et al., 1968; Lansbury, 1992). The most distinguishing characteristics of amyloid are its X-ray diffraction pattern, which is consistent with a cross-β structure, and its ability to form a complex with the dye Congo red which exhibits apple green birefringence when viewed in a polarized light source (Glenner, 1980; Kirschner et al., 1986, 1987; Jarvis et al., 1993; Fraser et al., 1994). The 16 currently known human amyloidogenic proteins have little sequence or structural homology, yet they all seem to be able to form a similar amyloid fibril structure (Kelly, 1996; Sipe, 1992, 1994). Our hypothesis is that the relatedness of these proteins is not at the level of their folded structures, but rather in their ability to adopt a common intermediate conformation upon partial denaturation which renders them capable of self-assembly into amyloid (Colon & Kelly, 1992; Kelly & Lansbury, 1994; Kelly, 1996). This hypothesis appears to be gaining experimental support, as recently conformational changes have been shown to be sufficient for conversion of the light chain (Hurle et al., 1994), β-peptide (Fraser et al., 1994; Simmons et al., 1994; Sorgehan et al., 1994; Howlett et al., 1995; Lee et al., 1995), transthyretin (Colon & Kelly, 1991, 1992; Gustavsson et al., 1991; McCutchen et al., 1993, 1995), and lysozyme (Pepys et al., 1993) into amyloid fibrils. Interestingly, a conformational change also appears likely for the conversion of Prp^{sol} into a prion-like particle in scrapie (Caughey et al., 1991; Prusiner, 1991; Pan et al., 1993; Safar et al., 1993, 1994; Come & Lansbury, 1994; Huang et al., 1994; Kocisko et al., 1994; Baldwin et al., 1995a,b; Bessen et al., 1995; Daggett, 1995; Goldfarb & Brown, 1995; Kocisko et al., 1995; Lansbury, 1995; Nguyen et al., 1995; Zhang et al., 1995). The means by which these conformational changes are achieved *in vivo* is still an unanswered question. One possibility is the acidic lysosomal organelles within cells through which many proteins pass during protein turnover. Our previous biophysical studies simulating the pH of a lysosome demonstrate that partial acid-mediated denaturation of TTR is sufficient for amyloid fibril formation *in vitro* (Colon & Kelly, 1992; McCutchen et al., 1993).

Lysosomes utilize acidic denaturation and proteolysis for protein degradation and are a possible site for amyloid fibril formation *in vivo*. Cohen, Glenner, and others have evidence that amyloid is present proximal to and inside lysosomes in reticuloendothelial cells in animals with amyloid disease (Glenner et al., 1971; Cohen et al., 1983). One reasonable scenario for the creation of amyloid from the amyloidogenic proteins in lysosomes is as follows. Amyloidogenic proteins selected for degradation/turnover are sent to the lysosome where the acidic environment effects partial acid denaturation and/or proteolysis, affording an amyloidogenic intermediate which can associate into amyloid fibrils at a rate competitive with normal degradation. Recycling of protease-resistant soluble pre-amyloid (assembled but not high enough molecular weight to be insoluble) and insoluble amyloid to the extracellular space may explain the location of amyloid deposits. It appears that amyloid in the extracellular space requires interactions with extracellular matrix components and other proteins for stability. It is likely that the majority of amyloid formed is catabolized by normal pathways; in fact, there is now good evidence for constant clearance of amyloid *in vivo*, even when the amyloid fibrils are stabilized by the interactions with other proteins (Tan et al., 1995). It appears that both denaturation-mediated amyloid formation and clearance pathways may be in delicate balance in normal individuals and become unbalanced in certain individuals, allowing amyloid to accumulate and become problematic. This paper is focused on understanding the tertiary and quaternary structural changes which facilitate acid-mediated transthyretin fibril formation with the long-term goal of understanding how to control the rate and extent of fibril formation *in vivo*. Identification of the structure of the transthyretin conformational intermediate (amyloidogenic intermediate) that is competent to self-associate into amyloid fibrils *in vitro* is a high priority.

MATERIALS AND METHODS

Transthyretin was purified from an *E coli* expression system described previously (McCutchen et al., 1993).

Purification involves liberating TTR and other proteins from the periplasmic space of *E. coli* through osmotic shock followed by a 8-fold concentration. The protein pellet produced by 70−85% ammonium sulfate precipitation is then subject to DEAE ion exchange chromatography, giving >95% purity. All studies reported in this paper utilize recombinant TTR, since TTR isolated from aged plasma is typically heterogeneous and not representative of the protein found *in vivo*, which is constantly turned over (Makover et al., 1988). The detergent Z 3-14 was obtained from Calbiochem. The Congo red used in these studies (Sigma) was recrystallized 2 times from water/ethanol by dissolving Congo red in water and crystallizing it by ethanol vapor diffusion. The vacuum-dried recrystallized Congo red was dissolved in 5 mM phosphate, 150 mM KCl, pH 7.5, and filtered 3 times through a 0.22 μm filter before it was used to evaluate the extent of fibril formation. The silver stain kit for PAGE gels was obtained from Sigma as was ANS which was used without further purification. Other reagents used were of highest purity available from Sigma or USB.

Amyloid Fibril Formation via Denaturation and Reconstitution. A 4−5 mg/mL TTR stock solution (10 mM phosphate, pH 7.4, 100 mM KCl, and 1 mM EDTA) was diluted into 50 mM sodium acetate or sodium phosphate buffered 100 mM KCl at the desired pH in an Eppendorf tube to obtain a final TTR concentration of 0.2 mg/mL to evaluate amyloid fibril formation via partial TTR denaturation. The resulting stationary solutions were incubated at 37 °C for 72 h before they were vortexed to equally distribute the fibrils, if present. The extent of fibril formation was probed by an optical density (OD) measurement at 330 nm in a standard UV cell (Andreu & Timasheff, 1986; Mulkerrin & Wetzel, 1989) and utilizing a quantitative Congo red binding assay. Adapting the procedure of Klunk et al., 50 μL of the vortexed TTR amyloid suspension was added to 1150 μL of a 10 μM Congo red solution (in 5 mM phosphate, 150 mM NaCl, pH 7.5) to provide an independent measurement of the mass of fibrils formed (Klunk et al., 1989; Glenner et al., 1974). The absorbance of the suspension at 477 and 540 nm was measured, and the amount of Congo red bound to amyloid fibrils is used to determine the quantity of fibrils in the suspension: mol of Congo red bound/L of amyloid suspension $= A_{540nm}/25\,295 - A_{477nm}/46\,306$. This method proved problematic and was not used for fibrils formed at pHs below pH 4.4 due to precipitation of Congo red. There is good agreement regarding the extent of fibril formation as a function of pH using both OD_{330} and the quantitative Congo red binding method (above pH 4.4). A time course of TTR amyloid fibril formation in the denaturation mode was carried out by diluting the TTR stock solution into acetate buffer at pH 4.4 using a single Eppendorf for each time point (Figure 2B). This method of fibril formation exhibits excellent reproducibility and is the method of choice for evaluating kinetics, inhibitors, etc. Reconstitution (renaturation)-induced amyloid fibril formation was also studied by first diluting a stock TTR solution into a pH 2.0 HCl solution with added 50 mM acetic acid, 100 mM KCl at 4 °C for ≥30 min to achieve "denaturation". This pH 2.0 solution was then incubated at 37 °C for 20 min before the pH was rapidly increased by adding a fixed amount of NaOH to bring the solution to desired pH. The final concentration of TTR was 0.2 mg/mL. The extent of fibril formation was evaluated by OD and Congo red binding as decribed above. To further demonstrate the integrity of the amyloid fibrils formed *in vitro* using the methods decribed above, the resulting fibrils were further studied by light and electron microscopy for comparison to authentic fibrils produced *in vivo*. For those samples exhibiting Congo red binding, the amyloid fibril−Congo red complex was viewed under a light microscope with a polarized light source to observe the expected apple green birefringence. Amyloid fibrils for electron microscopy evaluation were manipulated as described previously (Colon & Kelly, 1992; McCutchen et al., 1993). Briefly, dilute solutions of the amyloid fibrils were placed on carbon-coated copper grids, and allowed to stand for 2 min before the excess solution was removed. The grid was treated with fresh 1% uranyl acetate (pH 4.5) for 2 min. Excess staining solution was removed by filter paper blotting, affording negatively-contrasted TTR fibrils which were visualized using a Zeiss 10-C electron microscope as described previously (Colon & Kelly, 1992; McCutchen et al., 1993). The fibrils exhibited the characteristic dimensions reported previously (Colon & Kelly, 1992; McCutchen et al., 1993).

Probing the pH-Dependent Quaternary Structure Changes by SDS−PAGE. In order to monitor the quaternary structural changes that TTR undergoes during acid-induced denaturation, an SDS−PAGE method previously developed by our laboratory was used which facilitates measuring the fraction of tetramer and monomer present at a given pH using densitometry. When tetrameric TTR is incubated in SDS sample buffer at room temperature and loaded onto a SDS−PAGE gel, the tetramer dissociates and runs as a dimeric species, unlike monomeric TTR which migrates through the gel as expected (Colon & Kelly, 1992). The dimer band on the gel will faithfully represent the amount of tetramer present in solution as long as a dimeric species is not present in solution. The absence of dimeric intermediates in the pH-mediated denaturation of TTR was verified by glutaraldehyde cross-linking experiments which show only negligible amounts of dimeric TTR under the conditions used within (Colon & Kelly, 1992). Transthyretin (0.2 mg/mL) was incubated at 25 °C (37 °C would produce fibrils) in the appropriate buffer to establish the tetramer−monomer equilibrium as a function of pH. To prevent the refolding of an equilibrium mixture of tetramer and monomer at a given acidic pH upon neutralization required for gel loading, the micellar detergent Z 3-14 is added to the sample to achieve a final Z 3-14 concentration of 0.5 mg/mL. Control experiments outlined previously demonstrate that Z 3-14 does not allow reconstitution nor does it dissociate the tetramer present in the mixture; effectively, it prevents quaternary structural changes upon neutralization (Colon & Kelly, 1992). The quaternary structure stability of wild-type TTR as a function of pH was evaluated with samples incubated in 50 mM phosphate or acetate buffer, 100 mM KCl (25 °C) at the desired pH. The final TTR concentration was either 0.01 or 0.2 mg/mL, and the final sample volume was 200 μL. After 40−44 h, Z 3-14 from a 25 mg/mL stock was added to each solution to afford a final Z 3-14 concentration of 0.5 mg/mL. Afterward, 60 μL of a 0.6 M phosphate buffer containing 0.5 mg/mL Z 3-14 was added to each TTR solution to neutralize the sample. A 20 μL sample was removed from each Eppendorf tube and mixed with 10 μL of 5% SDS sample buffer. These unboiled samples were loaded onto a 12% SDS−PAGE gel which was stained either by Coomassie blue (0.2 mg/mL)

or by silver stain (0.01 mg/mL), and analyzed by a Molecular Dynamics Model 300A computing densitometer. The midpoint (pH_m) of the acid-mediated tetramer to monomer transition is the pH at which half of the TTR is in tetrameric form by weight. Figure 3 summarizes the SDS−PAGE experimental procedure for evaluating the pH-dependent quaternary structural changes exhibited by TTR.

Probing the pH-Dependent Quaternary Structure Changes by Analytical Equilibrium Ultracentrifugation. The weight-averaged molecular weights of TTR at pH 7.0, 5.05, 4.10, and 2.0 were obtained from data collected on a Beckman XL-A analytical ultracentrifuge with absorption optics. TTR solutions (0.2 mg/mL) at the desired pH (50 mM phosphate or acetate buffer) in 100 mM KCl were prepared and incubated at 4 °C for at least 12 h, and then brought up to 25 °C for another 12 h, except in the case of pH 2 sample where a 0.05 mg/mL solution was used. A double-sector cell equipped with a 12 mm Epon centerpiece and quartz windows was loaded with a blunt-end microsyringe, resulting in a column height of approximately 3 mm. Data monitoring the absorbance at 234 nm were collected at 25 °C, using a speed of 17 000 rpm and an average of 20 scans per point. A partial specific volume of 0.75 was determined by fitting the data to the expected molecular mass of 54 kDa at pH 7. This value is similar to that used previously by Branch (0.73) for their ultracentrifugation studies on TTR (Branch et al., 1971). It was assumed that the partial specific volume would not change significantly for monomeric TTR, which appears to be valid based on MW determinations under conditions known to give monomeric TTR in our laboratory and based on the earlier work of Branch.

pH-Dependent Far- and Near-UV Circular Dichroism. The CD spectra of TTR were recorded on an Aviv Model 62DS spectrometer at 25 °C using a bandwidth of 0.5 nm, a time constant of 2 s, and a step size of 0.2 nm employing 4 averages. TTR solutions (0.2 mg/mL) at the desired pH (50 mM phosphate or acetate buffer) in 100 mM KCl were prepared at 4 °C and incubated for 12 h, and then brought up to 25 °C for another 12 h, taking advantage of the observation that TTR does not aggregate at temperatures ≤25 °C (*vide supra*). The far-UV CD spectra were recorded from 196 to 250 nm using a 1 mm quartz cell whereas the near-UV CD spectra of the above solutions were recorded from 250 to 320 nm in a 2 cm quartz cell. All data are reported in units of mean residue ellipticity (Schmid, 1989). The far-UV CD spectra were smoothed using a Stineman function (KaleidaGraph software) which removed the noise without perturbing the appearance of the data. The near-UV CD data were reported without manipulation to preserve all the detail.

Acid Denaturation of TTR by Fluorescence Spectroscopy. Fluorescence measurements of TTR were recorded on a 8000 SLM Aminco fluorometer at 25 °C in a 1 cm path length quartz cell, using an excitation slit width of 4 nm and an emission slit width of 8 nm. The TTR samples made up at 0.01 mg/mL at the desired pH in 50 mM phosphate or acetate buffer, 100 mM KCl were incubated at 25 °C for 40−45 h, unless specified as being without added KCl. The excitation wavelength was set at 295 nm and the emission wavelength monitored at 340 nm to measure exclusively the tryptophan fluorescence. In another experiment, the excitation wavelength was set at 278 nm and emission at 340 nm to measure the tyrosine to tryptophan energy transfer via tryptophan fluorescence.

ANS Binding. A concentrated stock of ANS was made by dissolving ANS in water: the concentration was determined by its absorption at 351 nm ($\epsilon = 6240\ M^{-1}\ cm^{-1}$). Fluorescence spectra were obtained with an Aminco SLM 8100 spectrofluorometer in 1 cm path length quartz cells at 25 °C by photon counting methods with the excitation wavelength set at 410 nm and the emission spectra recorded from 420 to 600 nm. Both of the excitation slits were set at 2 nm, while the emission slits were set at 2 and 4 nm, respectively. Low TTR (0.01 mg/mL) and ANS (48 μM) concentrations were used such that the absorbance was less than 0.1 at both the excitation and emission wavelengths to minimize the inner filter effect. For the tryptophan to ANS energy transfer fluorescence spectra, 0.01 mg/mL TTR and 0−48 μM ANS were used. The excitation wavelength was set at 295 nm, and the emission spectra were recorded from 300 to 580 nm. The inner filter effect at 48 μM ANS was not corrected for since these data were not analyzed quantitatively.

To measure the binding of ANS to TTR as a function of pH, 3 mL of a 0.01 mg/mL TTR solution in buffers of differing pH containing 100 mM KCl was prepared and equilibrated at 25 °C for 40−44 h. An aliquot of an ANS stock solution was then added to each solution to make the final ANS concentration 48.0 μM. The resulting solutions were incubated for an additional 24 h, and fluorescence intensities were measured using an excitation wavelength of 410 nm and an emission wavelength of 490 nm. Fluorescence intensities reported were relative to that of a solution of TTR and ANS at pH 2.0. To evaluate the pH-dependent quaternary structure of TTR in the presence of ANS, samples prepared according to the above procedure were subjected to SDS−PAGE gel analysis described above (refer to the experimental section describing the determination of TTR quaternary structure by SDS−PAGE).

Probing Acid Denaturation of TTR Using Single Tryptophan Containing Variants. Two single tryptophan containing TTR mutants, Trp-41-Phe and Trp-79-Phe, were prepared utilizing site-directed mutagenesis as described previously (McCutchen et al., 1993, 1995). The extinction coefficients for W41F ($\epsilon_{280nm} = 54\ 781\ M^{-1}\ cm^{-1}$) and for W79F ($\epsilon_{280nm} = 51\ 300\ M^{-1}\ cm^{-1}$) were determined according to the method of Gill et al. (Gill & von Hippel, 1989). The SDS−PAGE quaternary analysis and fluorescence-monitored acid denaturation of these two mutants were carried out following the procedures described above. The fluorescence denaturation curves probe the proximity of each Trp to the acid-mediated structural rearrangement in TTR via their change in local environment.

RESULTS

Amyloid Fibril Formation. Transthyretin amyloid fibril formation was monitored by the turbidity at 330 nm and/or Congo red binding as a function of pH, both during acid denaturation and during pH-mediated reconstitution (Figure 2) in a stagnant assay. The amyloid-like structure of these aggregates was confirmed by Congo red binding and polarized microscopy, as well as by electron microscopy (Colon & Kelly, 1992; McCutchen et al., 1993, 1995). The amount of amyloid formed at pH 4.4 in the stagnant reconstitution-mediated process (Figure 2C) is greater than that formed in the stagnant denaturation mode of fibril

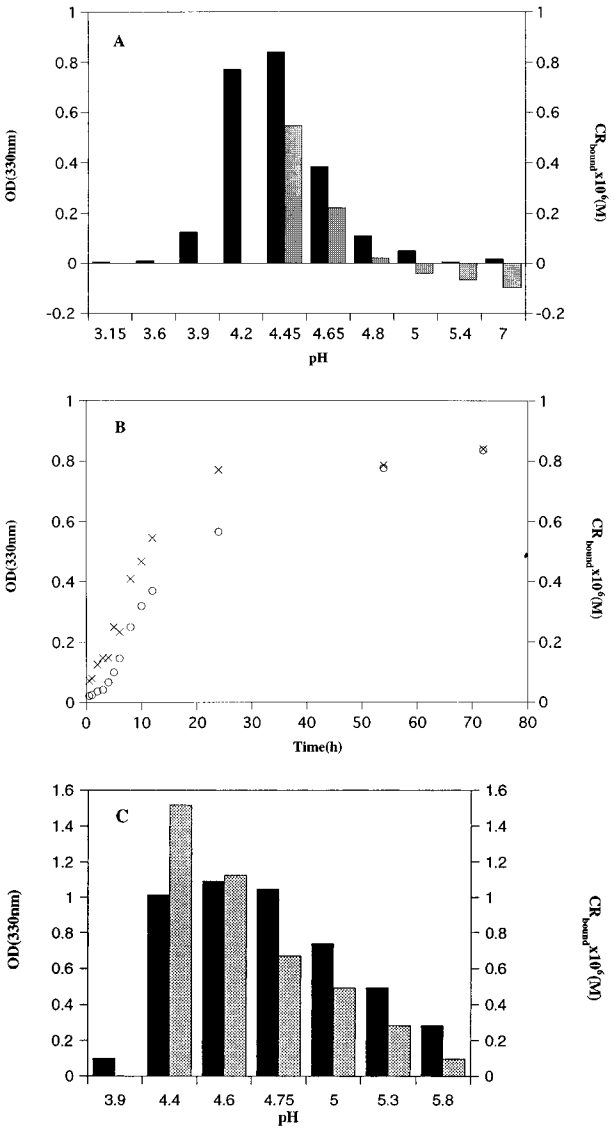

FIGURE 2: (A) Bar graph depicting the extent of TTR fibril formation after 72 h upon partial denaturation at the pHs indicated. Two methods were used for measuring the extent of fibril formation at each pH; the black bars represent the OD measurements while the lightly shaded bars represent the quantitative Congo red determinations. (B) Time course of TTR fibril formation facilitated by partial denaturation at pH 4.4. The extent of fibril formation was evaluated using both OD (○) and the quantitative Congo red method (×). (C) Bar graph depicting the extent of TTR fibril formation after 72 h upon reconstitution from the denatured state. Two methods were used for measuring the extent of fibril formation at each pH; the black bars represent the OD measurements while the lightly shaded bars represent the quantitative Congo red determinations.

formation (Figure 2A) at equal TTR concentrations (0.2 mg/mL), demonstrating that fibril formation occurs to a greater extent in the reconstitution mode. These results imply that a kinetic barrier exists between the amyloidogenic intermediate and the nonamyloidogenic tetramer during reconstitution, resulting in a higher concentration of the amyloidogenic intermediate. The pH associated with maximal fibril formation in both modes is observed to be near pH 4.4 (Figure 2A,C), close to the isoelectric point of TTR (4.6−4.95 for tetrameric TTR from human plasma; Pettersson et al., 1987). The mass of amyloid formed over a 3 day period as a function of pH in the stagnant assay was evaluated by optical density measurements and by determining the extent of Congo red binding, (Figure 2A,C). It was reassuring to see that the optical density and Congo red binding method generally agree on the relative mass of amyloid formed at a given pH. The observation of transthyretin amyloid fibril formation without stirring demonstrates that shear forces are not necessary for TTR fibril formation. A time course of TTR (0.2 mg/mL) fibril formation at pH 4.4 reveals what appears to be a nucleated condensation mechanism of fibril formation (Figure 2B). In this mechanism, several subunits must associate to form a nucleus in an energetically unfavorable process which is generally associated with a lag phase, as seen in the time course shown in Figure 2B. A cooperative growth phase is also observed where the addition of the amyloidogenic monomer to the growing fibril occurs with a favorable equilibrium constant. Fibril growth begins to plateau at ca. 50 h, consistent with depletion of the monomeric amyloidogenic intermediate below the critical concentration which is required for growth. A similar mechanism has also been shown to govern fibril formation of TTR isolated from plasma where a stirred solution was studied (Colon & Kelly, 1992).

Inhibiting TTR Fibril Formation—Facilitating Studies on the Denaturation Pathway. Since partial denaturation and amyloid fibril formation are competing processes, it is possible to identify the intermediates that partition into amyloid by carefully studying the acid denaturation pathway. To probe the denaturation pathway, it is necessary to inhibit fibril formation, which can be accomplished by lowering the protein concentration and/or the temperature. Since the self-assembly of a folding intermediate is at the minimum a second-order process, fibril formation during denaturation can be inhibited by studying the denaturation pathway at low transthyretin concentration (0.01−0.2 mg/mL) at 25 °C. On the upper end of the TTR concentration range (0.2 mg/mL), it is necessary to work at 25 °C instead of 37 °C to avoid fibril formation. The self-assembly of the amyloidogenic intermediate at 37 °C but not at 25 °C (0.2 mg/mL) is most likely a result of the temperature dependence of the hydrophobic effect (Dill, 1990).

TTR Quaternary Structural Changes Evaluated by SDS−PAGE and Analytical Equilibrium Ultracentrifugation. TTR exists as an equilibrium mixture of tetramer and monomer at acidic pHs as discerned from SDS−PAGE gel studies and analytical equilibrium ultracentrifugation data. Ultracentrifugation analysis gives a weight-averaged molecular mass of 54.4 kDa at pH 7, 51.1 kDa at pH 5.05, and 44.7 kDa at pH 4.1. Below pH 4, TTR aggregates in the centrifugation experiments carried out at 0.2 mg/mL, likely as a result of the centrifugal force which concentrates the sample at the bottom of the cell (similar behavior is not observed in the absence of centrifugal force). Therefore, 0.05 mg/mL TTR solutions were used at pH 2.0 in the ultracentrifuge, which gives an apparent mass of 17 kDa for the supernatant component in the cell (an estimated 30−40% of TTR still sedimented to the bottom of the cell). At physiological concentration (0.2 mg/mL), TTR exists primarily in tetrameric form from pH 7 to 5 according to SDS−PAGE and ultracentrifugation data. From pH 5 to pH 3.5, TTR undergoes a tetramer to monomer transition, with a midpoint around pH 4.3 (Figure 4), as determined by the SDS−PAGE method outlined in Figure 3. At pHs below 3, monomeric TTR is observed as discerned from SDS−PAGE analysis and analytical ultracentrifuge data. Transthyretin will not

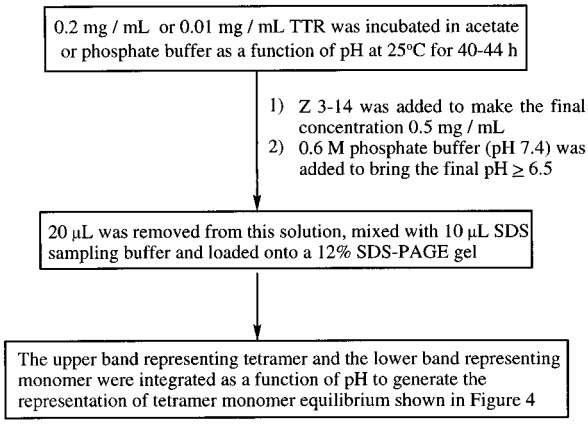

FIGURE 3: Flow chart summarizing the SDS−PAGE method used to evaluate the pH-dependent TTR quaternary structural changes.

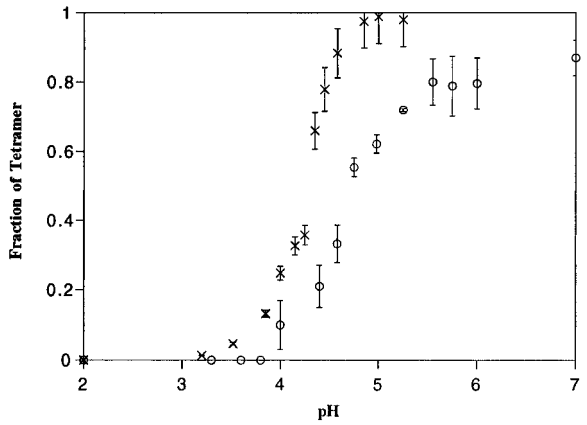

FIGURE 4: pH-dependent quaternary structural changes in wild-type TTR as a function of pH at two concentrations, 0.2 mg/mL (×) and 0.01 mg/mL (○). Samples were incubated at the desired pH for 40−44 h and manipulated as outlined in Figure 3. SDS−PAGE gels were scanned by densitometry to measure the relative amount of tetramer and monomer at each pH.

form fibrils or aggregate (no increase in OD) below pH 3.5 at 37 °C for 3 days (see Figure 2A), demonstrating that the aggregation observed in the ultracentrifuge is likely a result of the centrifugal force and is not representative of what occurs in solution. To further understand the denaturation curve detected by the fluorescence at 0.01 mg/mL, we also performed SDS−PAGE analysis of quaternary structural changes at a TTR concentration of 0.01 mg/mL. A comparison of the tetramer to monomer transitions of TTR as a function of concentration reveals that this transition is concentration-dependent: the lower the concentration of TTR, the more the tetramer−monomer equilibrium will be shifted toward monomer at a given pH (Figure 4). When a 0.01 mg/mL solution of TTR is incubated at 25 °C at pH 7.0, approximately 15% monomeric TTR is observed in solution. As the pH decreases, from pH 5.3 to pH 4, TTR undergoes a tetramer to monomer transition, the midpoint being around pH 4.7.

pH-Mediated Tertiary Structural Changes Monitored by Fluorescence Spectroscopy. The acid-mediated denaturation of wild-type TTR monitored by Trp fluorescence exhibits biphasic behavior (Figure 5). The fluorescence intensity over the pH range of 7−5.2 exhibits a fluctuating increase which may reflect a subtle tertiary structural rearrangement within tetrameric TTR. In the pH range of 5.2−4.3, the first significant tertiary structural transition is observed, which does not appear to be directly coupled to the tetramer to

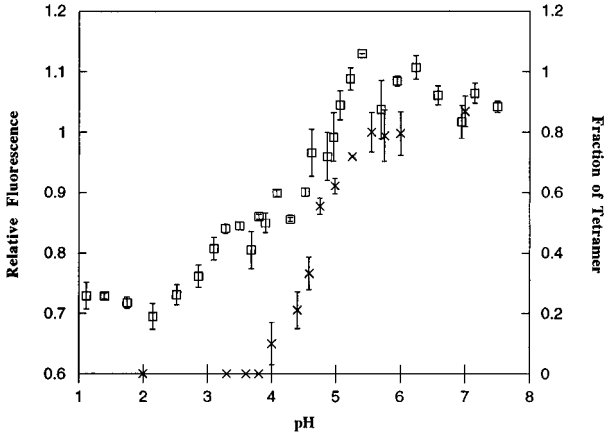

FIGURE 5: Acid denaturation curve of wild-type TTR (0.01 mg/mL) monitored by changes in the tryptophan fluorescence intensity (□) at 340 nm (excitation at 295 nm). The pH-dependent equilibrium between the tetramer and monomer as monitored by the SDS−PAGE method is shown (×) to aid in interpretation.

monomer quaternary structural transition, *vide infra*. Interestingly, a fluorescence plateau is observed from pH 4.3 to 3.3 which likely reflects the buildup of a steady-state concentration of an amyloidogenic intermediate(s) (McCutchen et al., 1995). This interpretation of the plateau in the fluorescence denaturation curve is consistent with the ability of TTR to make amyloid fibrils over the pH range of 5−3.9, albeit at a higher TTR concentration. The fluorescence plateau and fibril-forming pH ranges should not be exactly the same, for the TTR concentrations in these experiemnts are different. The fluorescence denaturation curve should not plateau until the monomer with an altered tertiary structure (amyloidogenic intermediate) is the predominant contributor. However, OD measurements can detect a relatively low concentration of the monomeric amyloidogenic intermediate because it can self-assemble into amyloid at pHs <5. Over the pH range of 3.5−2, a second significant transition is observed by Trp fluorescence, which appears to reflect the transition from a structured monomeric intermediate to a molten globule-like acid-denatured state (A-state), *vide infra*. As the pH is lowered from 7.0 to 2.0, the maximum emission wavelength of TTR only exhibits a slight red shift from 334 to 337 nm (McCutchen et al., 1995), indicating that the tryptophan residues in TTR are still buried in a nonpolar, but altered environment. The intensity is quenched by 30% at pH 2.0, which is likely to be due to dynamic quenching as a result of increased side chain mobility. The fluorescence-monitored denaturation of TTR appears to be rather insensitive to quaternary structural changes, based on the observation that amyloidogenic variants of TTR having single site mutations which destabilize tetrameric TTR exhibit similar fluorescence denaturation curves (McCutchen et al., 1995). This result implies that the fluorescence-based denaturation curves result largely from a rearrangement in the tertiary structure of TTR, which is clearly demonstrated in the studies on the W-79-F TTR variant discussed below. Fluorescence spectroscopy is expected to be rather insensitive to quaternary structural changes based on what has been described for other proteins in the literature, except in those cases where quaternary structural changes significantly alter the environment of one or more Trp residues (Fernando & Royer, 1992).

Fluorescence-Monitored Denaturation of W-79-F and W-41-F TTR—Probing the Location of the pH-Mediated

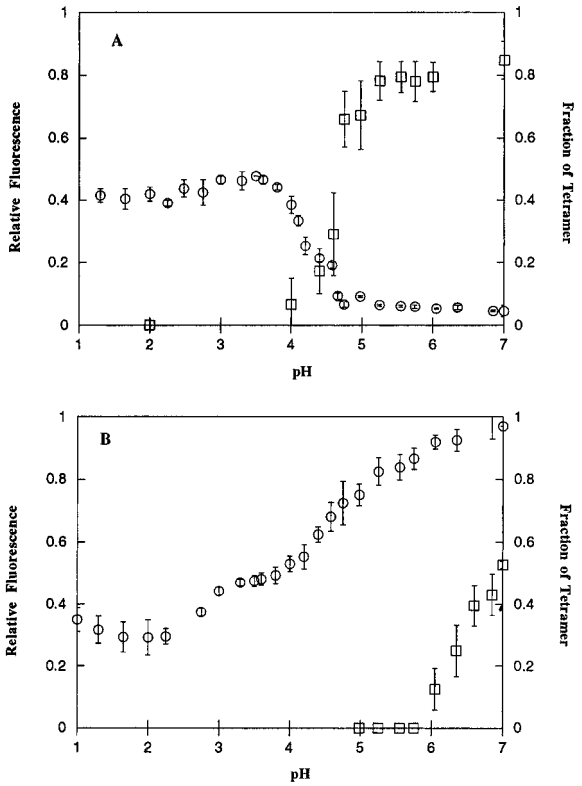

FIGURE 6: (A) Acid denaturation curve of the W-41-F TTR variant (0.01 mg/mL) monitored by changes in the Trp-79 fluorescence intensity at 340 nm (○). The pH dependent equilibrium between the tetramer and monomer as monitored by the SDS−PAGE method is shown (□) to aid in interpretation. (B) Analogous fluorescence denaturation curve of the W-79-F TTR variant exhibiting Trp-41 fluorescence at 340 nm (○) and pH-dependent tetramer−monomer equilibrium (□) for the W-79-F variant monitored by SDS−PAGE.

Tertiary Structural Rearrangement. TTR has two Trp residues in each of its four identical subunits. Fortunately, the Trp residues are located far apart in the TTR tertiary structure: W-79 is located in the helix intervening between strands E and F, and W-41 is in the loop proximal to the beginning of strand C (Figure 1). The fluorescence-monitored denaturation of the single Trp containing TTR variants (W-41-F and W-79-F) allows us to better understand the location of the pH-mediated tertiary structural changes in wild-type TTR which leads to the formation of the amyloidogenic intermediate. Interestingly, the W-41-F variant does not exhibit W-79 fluorescence over the pH range of 7−5, implying the presence of an intrinsic quencher in TTR's normally folded structure. This quencher is relocated relative to W-79 in the rearrangement occurring between pH 5 and 3.7 as discerned from increased W-79 fluorescence (Figure 6A). Below pH 3.7, the fluorescence of the W-79 is invariant, indicating that no further fluorescence-detectable changes in tertiary structure occur in this region of the molecule. The tetramer to monomer transition in the case of the W-41-F variant of TTR is largely centered between 5 and 4, leading one to speculate that the dissociation of the tetramer may relocate the quencher if the quencher is located in a different subunit. Alternatively, it may be a monomer rearrangement that relocates the Trp-79 relative to the quencher, assuming that the quencher is located in the same subunit. Since the tetramer−monomer transition and the fluorescence transition overlap (see Figure 6A), it cannot be stated with certainty which is the case at this time.

The W-79-F TTR variant exhibits a pH-mediated fluorescence denaturation curve with a wealth of information relative to the location of the tertiary structural rearrangement(s) in TTR. The pH-dependent tetramer to monomer transition (0.01 mg/mL) of W-79-F is overlaid on the pH-dependent fluorescence denaturation curve in Figure 6B. From these data, it is clear that the tetramer is dissociated into monomer almost completely at pH 6; yet the majority of the fluorescence changes occur at pHs <6, consistent with the literature consensus that fluorescence spectra predominantly monitor tertiary structural changes. It is interesting that the W-79-F mutation significantly destabilizes the tetramer, probably because the W-79 is located proximal to the AB loop which facilitates the dimer−dimer interaction to form the tetramer. The decrease in fluorescence from pH 7 to 5 is linear with decreasing pH, suggesting that Trp-41 is located in or near the portion of TTR that is undergoing a tertiary structural rearrangement. From pH 5.5 to 3.9, the change of fluorescence with pH is also linear, but the steeper slope suggests a more pronounced pH dependence, perhaps indicating a further rearrangement in this region within the monomer. Importantly, the W-79-F variant exhibits a plateau in fluorescence from pH 4.1 to 3, consistent with the formation of the amyloidogenic intermediate building up to a steady-state concentration. In support of this interpretation, the W-79-F variant readily makes amyloid over this pH range, albeit at higher concentrations. A second transition over the pH range of 3−2 is also evident for W-79-F, in accord with a structured monomer to A-state conformational change also exhibited by wild-type TTR, *vide supra*. The A-state is not capable of self-assembling into amyloid. The pH-dependent fluorescence denaturation curve of the W-79-F TTR variant, when considered in the context of pH-dependent TTR V8 protease sensitivity data emerging from this laboratory, is consistent with a rearrangement in TTR involving the C-strand−loop−D-strand region of TTR which is proximal to W-41 (Figure 1) (Miroy and Kelly, unpublished results). This rearrangement appears to occur in the monomer and possibly to a limited extent in the tetramer.

Far- and Near-UV CD of TTR as a Function of pH. To further evaluate the conformational changes occurring in TTR as a function of pH, far- and near-UV CD studies were employed to probe the secondary and tertiary structural changes, respectively. A series of pH-dependent far-UV CD spectra were obtained (Figure 7A). The far-UV CD spectra of TTR exhibit little change from pH 7.5 to pH 4.4. However, the signal at 215 nm, which reports on β-sheet content, displays an increase at pHs <4.4, possibly due to the attenuation of the aromatic contribution to the far-UV CD region upon tertiary structural changes (the aromatic contribution is usually positive in this wavelength range). It is important to keep in mind that there is approximately half TTR monomer and half tetramer at pH 4.4 (0.2 mg/mL) which complicates the interpretation of the CD spectra. A conservative interpretation of the far-UV CD data is that slight alterations in the secondary structure are occurring below pH 4.4. The data to follow below suggest that a secondary structural rearrangement in the C-strand−loop−D-strand portion of TTR is occurring and since this region is highly twisted to begin with it most likely makes an unpredictable contribution (perhaps positive) to the far-UV CD spectrum in the 215 nm region. The near-UV CD spectra of TTR, resulting from the asymmetric packing of the

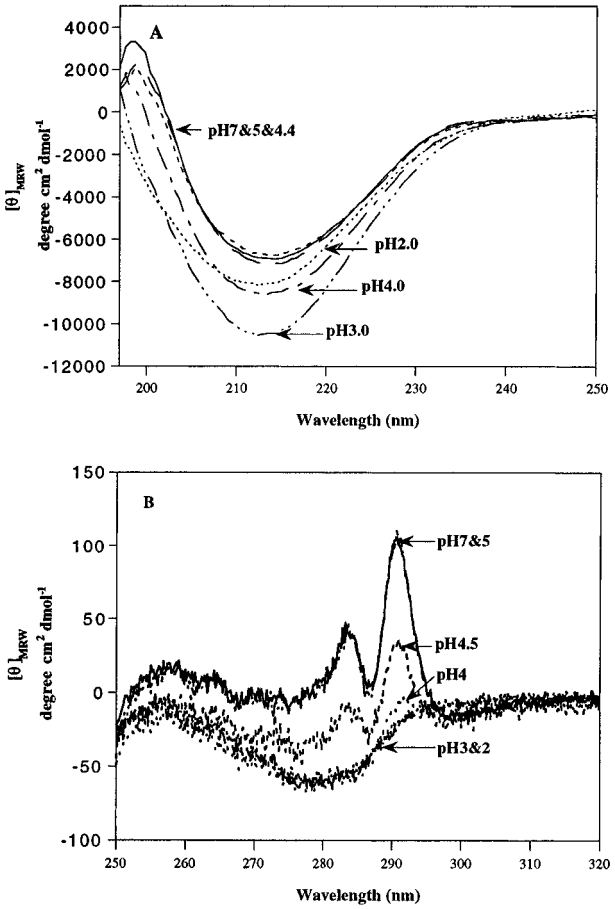

FIGURE 7: (A) Far- and (B) near-UV CD study of wild-type TTR at 0.2 mg/mL as a function of pH at 25 °C.

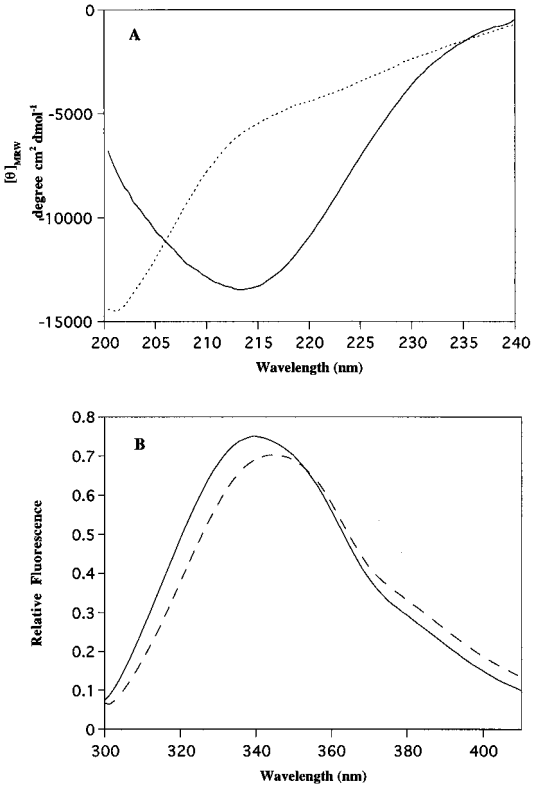

FIGURE 8: (A) Comparison of the far-UV CD spectra of wild-type TTR (0.2 mg/mL) in the presence (—) and absence (•••) of 0.1 M KCl at pH 2.0. (B) Tryptophan fluorescence spectra of TTR (0.01 mg/mL) in the presence (—) and absence (- - -) of 0.1 M KCl at pH 2.0, excitation at 295 nm.

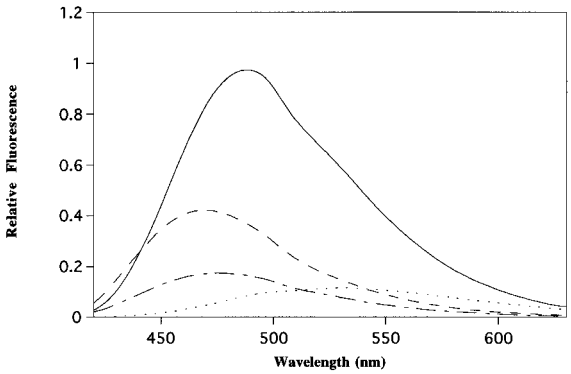

FIGURE 9: Comparison of ANS fluorescence in solution at pH 7 in the absence of TTR (•••) with ANS bound to TTR at pH 7 (— —), pH 4.4 (— - —), and pH 2 (—). ANS was excited at 410 nm.

tryptophan and tyrosine side chains, exhibit significant pH-dependent changes (Figure 7B). The near-UV CD signal from pH 7.5 to 5 exhibits little change, consistent with a largely unchanged tertiary structure over this pH range (Colon & Kelly, 1992). Two of the characteristic positive near-UV CD peaks, one at 283 nm and the other at 291 nm, become less intense over the amyloid-forming pH range of 5−4, implying a change in tertiary structure over this pH range (Woody, 1985; Buchner et al., 1991). Below pH 4, TTR exhibits negative ellipticity in the near-UV CD region which implies a rearranged and poorly defined tertiary structure consistent with its inability to make amyloid. The significant conformational changes leading to the amyloidogenic intermediate occur between pH 5 and 4, implying that the intermediate with a defined tertiary structure observed between pH 5 and 4 is the amyloidogenic intermediate.

The far-UV CD spectrum of TTR in HCl solution at pH 2 in the absence of salt exhibits a minimum at 200 nm, which is characteristic of a random coil (largely unstructured) conformation (Figure 8A). The absence of added chloride ions to bind and neutralize the ammonium groups creates a high positive charge density in TTR facilitating chain unfolding. The retention of secondary structure at pH 2 in the presence of added salt and the loss of structure upon addition of HCl without added salt are characteristic of the behavior of many proteins, which adopt an A-state-like conformation at low pH (Goto & Fink, 1989; Goto et al., 1990a,b; Fink et al., 1994). Unfolding of TTR under acidic low-salt conditions is further supported by the trytophan fluorescence emission maximum at 345 nm with reduced intensity when compared to the more intense fluorescence emission maximum at 337 nm in the A-state conformation (with added KCl). The 8 nm red shift and quenching strongly support greater solvent exposure of the Trp residues in the absence of added KCl (Figure 8B).

ANS Binding. Figure 9 shows spectra of a solution of ANS and TTR at pH 7, pH 4.4, and pH 2 compared to ANS alone at pH 7 (the fluorescence spectrum of ANS alone at pH 2 is very similar to the pH 7 spectrum shown). Pronounced increases in the intensity of ANS fluorescence as well as a shift of the fluorescence maximum to shorter wavelengths are observed when ANS binds to TTR. When ANS binds to TTR at pH 7, the maximum wavelength of ANS emission shifts from 525 nm (free) to 470 nm (bound), and exhibits

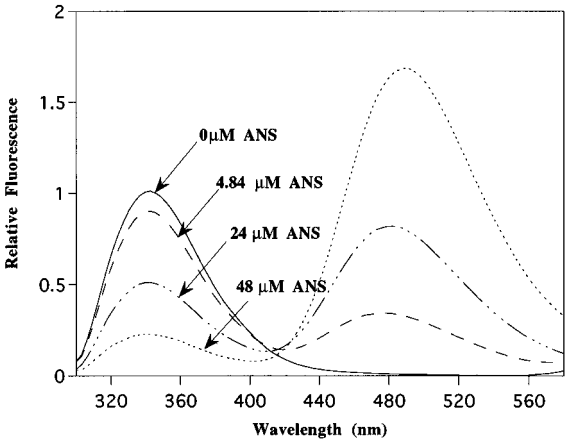

FIGURE 10: Tryptophan to ANS energy transfer study as a function of increasing ANS added to TTR at pH 2. The Trp residues were excited at 295 nm and emit at 340 nm in the absence of added ANS. Energy transfer to ANS is observed by ANS fluorescence from 440 to 570 nm.

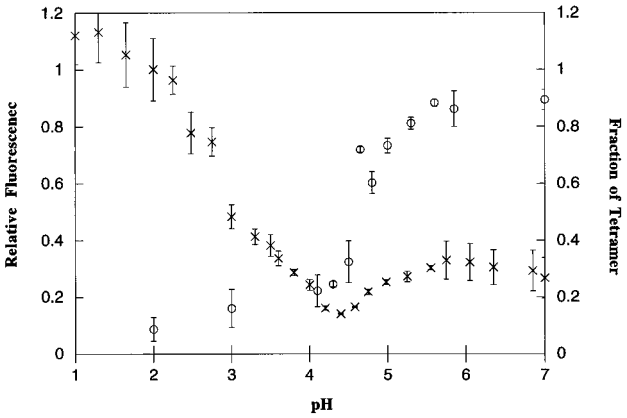

FIGURE 11: ANS (48 μM) binding to TTR (0.01 mg/mL) as a function of pH monitored by ANS fluorescence. Dissociation of the TTR tetramer to monomer as a function of pH in the presence of ANS (48 μM) is shown (○) as monitored by the SDS−PAGE method.

a 10-fold increase in intensity, consistent with the binding of ANS to the hydrophobic channel in TTR. Robbins et al. analyzed thyroid hormone binding to TTR employing ANS fluorescence and found that at pH 7.4 2 mol of ANS binds to 1 mol of tetrameric TTR (Cheng et al., 1977). The ANS and thyroxin binding sites overlap in the central channel formed by the association of the four subunits. At pH 2.0, ANS binds to monomeric TTR, leading to a large increase in fluorescence intensity as well as a further red shift to 490 nm when compared to the 470 nm (bound) emission maxima at pH 7. This suggests that ANS binds to TTR at pH 7 and pH 2 at different sites. At pH 2 under physiological salt conditions, TTR adopts an A-state conformation in solution, which exhibits native-like secondary structure, as determined by far-UV CD, but lacks native tertiary structure as discerned by the near-UV CD spectral changes. The fact that TTR binds to ANS at pH 2 and exhibits greatly enhanced ANS fluorescence intensity further supports the assignment of the pH 2 conformation to an A-state (Fink et al., 1994). Titration of TTR at pH 2 with ANS and titration of a fixed amount of ANS with an increasing concentration of TTR yield a Scatchard plot for ANS binding which was not linear, indicating multiple binding sites with different affinities. Double-reciprocal analysis gave an apparent dissociation constant of 200 μM and the number of ANS molecules bound as approximately 50 (Horowitz & Criscimagna, 1985). These data suggest that there is a large hydrophobic surface area exposed at pH 2 which can bind numerous ANS molecules. To study the binding of ANS to the acid-denatured state of TTR at pH 2, energy transfer experiments were performed with increasing amounts of ANS (Figure 10) relative to TTR. The intensity of the intrinsic fluorescence of tryptophans diminishes in parallel with the increasing ANS emission intensity. This demonstrates that the quenching of the tryptophan fluorescence is due to ANS binding and that some ANS binding sites are in close proximity to one or both of the tryptophans in TTR. Now that the binding of ANS to the nonamyloidogenic intermediates formed at the extremes of pH used in this study is understood, focus was turned to the intermediates populated between these limits.

1-Anilino-8-naphthalenesulfonate binding to TTR as a function of pH was employed to follow denaturation and to evaluate the relative hydrophobicity of the amyloidogenic intermediate (Figure 11). The first transition is observed over the pH range of 5.5−4.4. Since the binding of ANS to TTR at neutral pH occurs in the central channel formed by the TTR tetramer, the reduction in ANS binding as the pH is lowered is consistent with a increasing monomer population which apparently cannot bind ANS with high affinity. This was confirmed by directly monitoring the tetramer to monomer transition by the SDS−PAGE method described here with TTR solutions preincubated at various pHs, followed by the addition of ANS 40 h later (Figure 11). At pH 4.4, the majority of tetrameric TTR is dissociated into monomer as discerned from the reduced ANS binding and the SDS−PAGE analysis. Interestingly, the monomeric conformer of TTR formed at pH 4.4 (80% monomer based on SDS−PAGE analysis) does not bind to ANS as strongly as TTR at pH 2 or at pH 7, consistent with an amyloidogenic intermediate that retains most of its tertiary structure and has properties of a structurally defined protein. Importantly the pH associated with maximal amyloid fibril formation (pH 4.4) exhibits a minimum in ANS binding, demonstrating that the amyloidogenic intermediate is not markedly hydrophobic and is certainly not molten-globule-like. When the pH is lowed below 4, the ANS fluorescence intensity increases considerably due to the increased hydrophobic surface area exposed upon rearrangement of the structured monomeric amyloidogenic intermediate to an A-state-like conformation. The fluorescence emission maximum of ANS bound to TTR at pH 4.4 is at 480 nm, which lies in between that of ANS bound to TTR at pH 7 (470 nm) and ANS bound to TTR at pH 2 (490 nm) (Figure 9). The 480 nm emission from the predominantly monomeric TTR amyloidogenic intermediate at pH 4.4 suggests that the ANS binding site(s) on TTR at pH 4.4 is (are) more hydrophobic than the binding sites at pH 2, but less hydrophobic than the channel which binds 2 mol of ANS in the tetramer at pH 7.

DISCUSSION

The earlier observation by our laboratory that partial denaturation is sufficient to populate a conformational intermediate that can self-assemble into transthyretin amyloid *in vitro* has since proven to be general for several immunoglobulin light chain and lysozyme variants (Hurle et al., 1994; Pepys et al., 1993). Transthyretin amyloid fibril formation

is observed during both pH-induced denaturation and reconstitution. The optimum pH for fibril formation is around pH 4.4 in both cases, suggesting that acid denaturation and reconstitution from denatured TTR proceed through a common conformational intermediate (amyloidogenic intermediate) which self-associates into amyloid. Fibril formation affected by reconstitution (0.2 mg/mL at 37 °C) versus that mediated by denaturation (0.2 mg/mL, 37 °C) yields more fibrils, implying that the reconstitution mode is more efficient. During reconstitution (pH jump from 2 to 4.4), TTR refolds from the A-state (denatured state) to an amyloidogenic intermediate which can only progress further along the reconstitution pathway via a step with high activation energy. Thus, TTR falls into a kinetic trap where the amyloidogenic intermediate concentration builds up and forms amyloid in competition with the normal reconstitution pathway to tetramer. The time course of TTR fibril formation employing the denaturation-mediated approach (Figure 2B) is consistent with a nucleated condensation polymerization where a nucleus is formed in an energetically unfavorable step, followed by a rapid energetically favorable growth step which affords the amyloid fibrils.

The generality of denaturation-induced amyloid fibril formation has led us to study the denaturation pathway and amyloidogenicity of TTR in detail using a variety of biophysical methods to better understand the transthyretin amyloidogenic intermediate. It is reasonable to expect that the core structure of the TTR amyloidogenic intermediate will be representative of core structures of other amyloidogenic intermediates, since the structure of amyloid derived from the 16 known human amyloidogenic proteins appears to be very similar based on X-ray diffraction analysis (Kelly, 1996). The ability of these proteins to populate a common amyloidogenic intermediate core structure upon partial denaturation may be the common link between the human amyloidogenic proteins, which do not have apparent primary or tertiary structure homology. This hypothesis implies that there are subtle similarities in the linear sequences of the amyloidogenic proteins which scientists cannot yet appreciate (Kelly, 1996).

Identification of the TTR amyloidogenic intermediate is complicated by the fact that fibril formation occurs over a pH range where an equilibrium mixture of tetrameric and monomeric TTR exists at physiological concentrations. Analytical equilibrium ultracentrifugation results, SDS−PAGE analysis, the X-ray crystallography work of Blake, and also the ANS and thyroxin binding data all support a tetrameric predominantly β-sheet structure for TTR at pH 7.5. As the pH of the tetramer is decreased to ≈pH 5, the transthyretin tetramer begins to dissociate (Figure 4). Far- and near-UV CD indicates that the secondary structure and tertiary structure are wild-type-like down to pH 5 (0.2 mg/mL), indicating the retention of native-like structure in the tetramer under these conditions (Figure 7). The tetramer appears to be incapable of amyloid fibril formation based on the observation that whenever the TTR tetramer is exclusively populated, fibril formation is not observed. This is true in the case of several TTR amyloidogenic variants studied previously (data not shown here) exhibiting decreased stabilities relative to wild-type TTR such that amyloid fibril formation is observed at a much higher pH than with wild-type TTR because the amyloidogenic intermediate can be formed at a higher pH. It is not sufficient simply to have dissociation to a monomeric intermediate having native-like tertiary structure; both dissociation and a tertiary structural rearrangement are necessary as shown by a Y78L TTR variant which is predominantly monomeric at pH 7, but will not form fibrils until the tertiary structure is altered by lowering the pH slightly (Z. Lai, unpublished results). Additional evidence against tetrameric TTR as the amyloidogenic intermediate is that tetrameric TTR is resistant to SDS denaturation (runs as a dimer in an SDS−PAGE) but the fibrils themselves are SDS-sensitive (dissociate to a monomer in an SDS gel) (McCutchen & Kelly, 1993). This result implies that the conformation of TTR composing the amyloid fibril is different than that observed in the tetramer.

In all cases studied thus far, transthyretin amyloid begins to form when the tetramer starts to dissociate to a monomeric species having an altered tertiary structure. As the pH of the TTR solution (0.2 mg/mL) is decreased below pH 5.0, the tetramer begins to dissociate to the monomeric amyloidogenic intermediate which can partition into amyloid or remain soluble and monomeric until ≈ pH 4 depending on the concentration and temperature. The range and exact midpoint (pH_m) of the pH mediated tetramer to monomer transition are concentration dependent as expected (Figure 4). A 20-fold concentration difference (0.2 vs 0.01 mg/mL) lowers the pH_m of the more concentrated sample by 0.4 pH unit, which is quite significant (makes the tetramer more resistant to dissociation). Amyloid formation during TTR pH-mediated denaturation is favored by high (physiological) concentrations (≥0.2 mg/mL) and physiological temperature (37 °C). The self-assembly of the amyloidogenic intermediate is very sensitive to temperature; effectively no amyloid is formed at 25 °C (0.2 mg/mL), where we carry out spectroscopic studies to evaluate the denaturation pathway, presumably as a result of the temperature dependence of the hydrophobic effect (Dill, 1990). Interestingly, ANS binding probed by fluorescence is at a minimum at pH 4.4 [TTR is predominantly monomeric at the 0.01 mg/mL concentration used for fluorescence (pH 4.4)], indicating that the monomeric amyloidogenic intermediate that appears to build up to a steady-state concentration has a defined tertiary structure with minimal hydrophobic surface area exposed (Figure 11). The plateau in the pH-dependent Trp fluorescence denaturation curve (Figures 5 and 6) also supports the buildup of a steady-state concentration of the amyloidogenic intermediate over the amyloid-forming pH range. Because fluorescence is being carried out at a much lower concentration (0.01 mg/mL) where TTR is >80% monomeric, contributions from the nonamyloidogenic tetramer are not substantive, making the resulting interpretation easier than in the case of CD, for example, where different quaternary forms complicate interpretation. The Trp fluorescence transition preceding this plateau (Figure 5) is indicative of tertiary structural changes within the native TTR fold as depicted in Figure 1. The tertiary structural changes leading to the amyloidogenic intermediate are also strongly supported by the near-UV CD spectra at pH 4.4 (pH of maximal fibril formation at 37 °C), which suggests a slightly altered tertiary structure (Figure 7B). The far-UV CD spectra of TTR at pH 4.4 indicate native-like secondary structure for the amyloidogenic intermediate, implying that the rearrangement either is conservative in secondary structure content or involves regions not having a regular secondary structure to begin with (Figure 7A). The extent of fibril formation

decreases markedly below pH 3.9 (0.2 mg/mL), consistent with the loss of tertiary structure in the TTR monomer as seen in the near-UV CD spectrum (Figure 7B). These data collectively indicate that the amyloidogenic intermediate is a monomeric structurally well-defined β-sheet having a near-native tertiary structure. The dimeric state has never been observed to be significantly populated over the amyloid-forming pH range (by glutaraldehyde cross-linking studies etc.), but the tetramer almost certainly dissociates to the dimer first and then to the monomer (Jaenicke & Rudolph, 1986; Jaenicke, 1987). However, since its steady-state concentration is always low, it is hard to envision how the dimer could play a role in an intermolecular association process like amyloid fibril formation.

The fluorescence denaturation curves for single Trp containing transthyretin variants (W-41-F and W-79-F), where these Trp residues are far apart in the native tertiary structure, prove to be very useful in identifying regions of TTR that rearrange in going from the native structure to the monomeric amyloidogenic intermediate structure having an altered tertiary structure. The fluorescence spectrum of the W-79-F variant is particularly useful (Figure 6B) in that it strongly suggests that Trp-41 is in or close to the portion of transthyretin that undergoes this tertiary structural rearrangement as the pH is decreased. Significantly, the pH-dependent fluorescence curve derived from the single Trp-41 residue appears to be primarily responsible for the denaturation curve exhibited by wild-type TTR (compare Figures 5 and 6B). This observation implies that the conformational changes occurring in the W-79-F mutant also occur in the wild-type protein. These data and other pH-dependent proteolysis sensitivity data emerging from the laboratory suggest that the C-strand−loop−D-strand region of TTR undergoes a rearrangement between pH 5.1 and 4, leading to what appears to be a monomeric amyloidogenic intermediate having strands A, B, F, and H exposed (Figure 12). Careful inspection of the structure of TTR reveals that the exterior strands C and D, which are part of a contiguous sequence, interact weakly (few H-bonds and hydrophobic contacts) with the core β-sheet of TTR such that mild denaturing conditions could convert the C-strand−loop−D-strand region into a large unstructured region exposing the A and B strands in the monomer (Figure 12). Hence, the simplest reasonable working model of the monomeric amyloidogenic intermediate would be to assume that it is similar to the wild-type tertiary structure except that the C-strand−loop−D-strand region is displaced from the core of the protein in an unordered conformation. This model is strongly supported by the fragments found in human amyloid fibrils where cleavage is observed to occur in the C-strand−loop−D-strand regions *in vivo* (Gustavsson, 1995). This model is also consistent with all spectroscopic data collected to date.

Monomeric wild-type TTR is incapable of fibril formation below pH 3.9, most likely due to a loss of tertiary structure which is observed in the near-UV CD spectrum (Figure 7B). This loss of tertiary structure is also supported by the second (low pH) transition in the Trp fluorescence denaturation curve (Figure 5) as well as the observed increase in ANS binding detected by fluorescence, indicating that an A-state is forming at pH 2 (Figure 11). TTR exists in an A-state conformation stabilized by anion (Cl^-) binding with native-like secondary structure, as discerned from the far-UV CD spectrum, and non-native tertiary structure exhibited by the near-UV CD

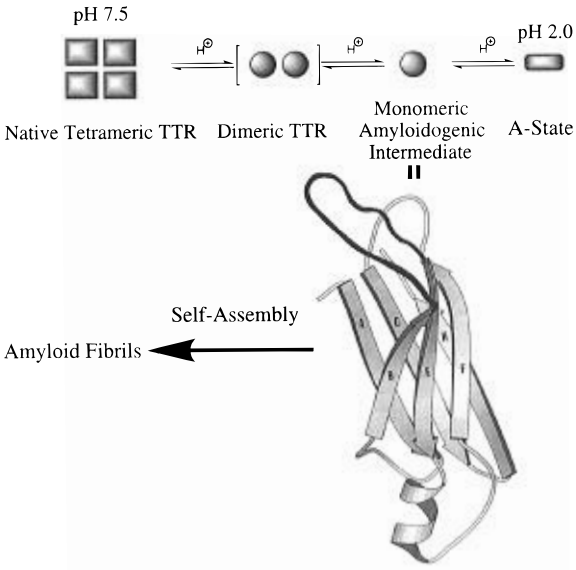

FIGURE 12: Summary of the acid denaturation pathway of wild-type TTR based on our current biophysical data. The structural model of the amyloidogenic intermediate shown is consistent with the data obtained thus far and is structurally very closely related to the tertiary structure of TTR at pH 7.5 in the tetramer (Figure 1).

spectrum at pH 2. The A-state ANS emission spectrum exhibits a red shift (from 470 to 490 nm) relative to the ANS emission when bound to TTR at pH 7, implying more solvent exposure of the ANS binding sites. In the absence of added salt, the β-sheet secondary structure of TTR is largely lost at pH 2.0 as discerned by the random coil far-UV CD spectrum (Figure 8A). A significant red shift in the tryptophan emission maximum of TTR to 345 nm is also consistent with further unfolding of TTR in the absence of added anions. Goto and Fink have shown that several proteins adopt an A-state conformation, which is characterized by a native-like secondary structure and a non-native tertiary structure at low pH in the presence of added salt. Anion binding to the ammonium groups appears to be the key factor for the formation of the compact acid-denatured state (A-state).

From the data presented within, it is very clear that acid-induced denaturation of TTR is not a two-state transition, even though tetramer and monomer comprise the vast majority of the quaternary species present at a given pH. Our current understanding of the transthyretin denaturation pathway is summarized in Figure 12. At physiological concentrations, tetrameric TTR remains associated from pH 7 to pH 5 and is incapable of amyloid fibril formation. Tetrameric TTR dissociates to a monomer in a process that is dependent on both pH and protein concentration below pH 5. The extent of amyloid fibril formation correlates with the concentration of the TTR monomer having an altered, but defined, tertiary structure over the pH range of 5.0−3.9 (Figure 12). The structurally defined monomeric amyloidogenic intermediate begins to adopt alternative conformations around pH 4 that are not amyloidogenic, ultimately forming an A-state conformation below pH 3 which is also not amyloidogenic.

Branch et al. studied the conformation of TTR in aqueous solutions in the early 70's and concluded that there were no significant changes in the tertiary structure of TTR between pH 3.5 and pH 12 based on UV, fluorescence, fluorescence anisotropy, circular dichroism, and analytical equilibrium

ultracentrifugation data (Branch et al., 1971). The acid-mediated denaturation curve monitored by Trp fluorescence recorded by Branch et al. is in good agreement with our own, and by today's standard implies significant tertiary structural changes. Their fluorescence anisotropy data collected on DNS-modified TTR are likely to be misleading with regard to the lack of perceived pH-induced structural changes because the DNS label is in a very flexible N-terminal region of the protein to begin with. The changes they observed in the CD and UV spectra were ascribed to quaternary structural changes; however, we now know that this is only partly true. In summary, most of Branch's data agrees with our own; however, their interpretation was based on what was known in 1971 and would undoubtedly be much different today.

Summary. The acid denaturation of pathway of TTR is characterized by several different intermediates having variable quaternary, tertiary, and secondary structures. Tetrameric TTR dissociates to a monomer in a process that is dependent on both pH and protein concentration below pH 5. The extent of amyloid fibril formation observed correlates with the concentration of the TTR monomer having a defined, but non-native tertiary structure. Further denaturation of TTR leads to an A-state which is not amyloidogenic. The biophysical data presented on the wild-type and single Trp containing TTR variants indicate that TTR rearranges in the C-strand−loop−D-strand region such that a monomeric β-sheet sandwich is afforded having the A, B, F, and H strands exposed which is capable of self-assembly into amyloid (Figure 12). Our improving understanding of the structure of the amyloidogenic intermediate and the mechanism of amyloid formation should make it possible to test therapeutic strategies for intervention in systemic amyloid diseases.

ACKNOWLEDGMENT

We are grateful to Thomas O. Baldwin and Greta Miroy for technical advice and many helpful discussions and Arthur Johnson and his group for many helpful discussions regarding fluorescence.

REFERENCES

Andreu, J. M., & Timasheff, S. N. (1986) in *Methods in Enzymology*, Academic Press, New York.

Baldwin, M. A., Cohen, F. E., & Prusiner, S. B. (1995a) *J. Biol. Chem. 270*, 19197−19200.

Baldwin, M. A., Pan, K. M., Nguyen, J., Huang, Z., Groth, D., Serban, A., Gasset, M., Mehlhorn, I., Fletterick, R. J., & Cohen, F. E. (1995b) *Philos. Trans. R. Soc. London, Ser. B: Biol. Sci. 343*, 435−441.

Benson, M. D. (1989) *Trends Biochem. Sci. 12*, 88−92.

Benson, M. D., & Wallace, M. R. (1989) in *The Metabolic Basis of Inherited Disease*, p 2439, McGraw-Hill, New York.

Bessen, R. A., Kocisko, D. A., Raymond, G. J., Nandan, S., Lansbury, P. T., & Caughey, B. (1995) *Nature 375*, 698−700.

Blake, C. C. F., Geisow, M. J., Swan, I. D. A., Rerat, C., & Rerat, B. (1974) *J. Mol. Biol. 88*, 1−12.

Blake, C. C. F., & Oatley, S. J. (1977) *Nature 268*, 115−120.

Blake, C. C. F., Geisow, M. J., & Oatley, S. J. (1978) *J. Mol. Biol. 121*, 339−356.

Branch, W. T., Robbins, J., & Edelhoch, H. (1971) *J. Biol. Chem. 246*, 6011−6018.

Buchner, J., Renner, M., Lilie, H., Hinz, H., & Jaenicke, R. (1991) *Biochemistry 30*, 6922−6929.

Caughey, B. W., Dong, A., Bhat, K. S., Ernst, D., Hayes, S. F., & Caughey, W. S. (1991) *Biochemistry 30*, 7672−7680.

Cheng, S. Y., Pages, R. A., Saroff, H. A., Edelhoch, H., & Robbins, J. (1977) *Biochemistry 16*, 3707−3713.

Cohen, A. S., & Calkins, E. (1959) *Nature 183*, 1202−1203.

Cohen, A. S., Shirahama, T., Sipe, J. D., & Skinner, M. (1983) *Lab. Invest. 48*, 1−4.

Colon, W., & Kelly, J. W. (1991) in *Applications of Enzyme Biotechnology* (Kelly, J. W., & Baldwin, T. O., Eds.) pp 99−108, New York.

Colon, W., & Kelly, J. W. (1992) *Biochemistry 31*, 8654−8660.

Come, J. H., & Lansbury, P. T., Jr. (1994) *J. Am. Chem. Soc. 116*, 4109−4110.

Cornwell, G. G., Sletten, K., Johansson, B., Westermark, P. (1988) *Biochem. Biophys. Res. Commun. 154*, 648−653.

Daggett, V. (1995) *Chem. Biol. 2*, 305−315.

Dill, K. A. (1990) *Biochemistry 29*, 7133−7155.

Divino, C. M., & Schussler, G. C. (1990) *J. Biol. Chem. 265*, 1425−1429.

Eanes, E. D., & Glenner, G. G. (1968) *J. Histochem. Cytochem. 16*, 673−677.

Fernando, T., & Royer, C. (1992) *Biochemistry 31*, 3429−3441.

Fink, A. L., Calciano, L. J., Goto, Y., Kurotsu, T., & Palleros, D. (1994) *Biochemistry 23*, 12504−12511.

Fraser, P. E., McLachlan, D. R., Surewicz, W. K., Mizzen, C. A., Snow, A. D., Nguyen, J. T., & Kirschner, D. A. (1994) *J. Mol. Biol. 244*, 64−73.

Furuya, H., Saraiva, M. J. M., Gawinowicz, M. A., Alves, I. L., Costa, P. P., Sasaki, H., Goto, I., & Sakaki, Y. (1991) *Biochemistry 30*, 2415−2421.

Gill, S. C., & von Hippel, P. H. (1989) *Anal. Biochem. 182*, 319−326.

Glenner, G. G. (1980) *N. Engl. J. Med 302*, 1283−1292.

Glenner, G. G., Ein, D., Eanes, E. D., Bladen, H. A., Terry, W., & Page, D. L. (1971) *Science 174*, 712−714.

Glenner, G. G., Eanes, E. D., Bladen, H. A., Linke, R. P., & Termine, J. D. (1974) *J. Histochem. Cytochem. 22*, 1141−1158.

Goldfarb, L. G., & Brown, P. (1995) *Annu. Rev. Med. 46*, 57−65.

Goto, Y., Calciano, L. J., & Fink, A. L. (1990a) *Proc. Natl. Acad. Sci. U.S.A. 87*, 573−577.

Goto, Y., & Fink, A. L. (1989) *Biochemistry 28*, 945−952.

Goto, Y., Takahashi, N., & Fink, A. L. (1990b) *Biochemistry 29*, 3480−3488.

Gustavsson, Å., Engstrom, U., & Westermark, P. (1991) *Biochem. Biophys. Res. Commun. 175*, 1159−1164.

Gustavsson, Å., Jahr, H., Tobiassen, R., Jacobson, D. R., Sletten, K., & Westermark, P. (1995) *Lab. Invest. 73*, 703−708.

Hamilton, J. A., Steinrauf, L. K., Braden, B. C., Liepnieks, J., Benson, M. D., Holmgren, G., Sandgren, O., & Steen, L. (1993) *J. Biol. Chem. 268*, 2416−2424.

Horowitz, P. M., & Criscimagna, N. L. (1985) *Biochemistry 24*, 2587−2593.

Howlett, D. R., Jennings, K. H., Lee, D. C., Clark, M. S. G., Brown, F., Wetzel, R., Wood, S. J., Camilleri, P., & Roberts, G. W. (1995) *Neurodegeneration 4*, 23−32.

Huang, Z., Gabriel, J. M., Baldwin, M. A., Fletterick, R. J., Prusiner, S. B., & Cohen, F. E. (1994) *Proc. Natl. Acad. Sci. U.S.A. 91*, 7139−7143.

Hurle, M. R., Helms, L. R., Li, L., Chan, W., & Wetzel, R. (1994) *Proc. Natl. Acad. Sci. U.S.A. 91*, 5446−5450.

Jaarsveld, P. P. V., Edelhoch, H., Goodman, D. S., & Robbins, J. (1973) *J. Biol. Chem. 248*, 4698−4705.

Jacobson, D. R., & Buxbaum, J. N. (1991) *Adv. Hum. Genet. 20*, 69−123.

Jaenicke, R. (1987) *Prog. Biophys. Mol. Biol. 49*, 117−237.

Jaenicke, R., & Rudolph, R. (1986) in *Methods in Enzymology*, pp 218−250, Academic Press, New York.

Jarvis, J. A., Craik, D. J., & Wilce, M. C. (1993) *Biochem. Biophys. Res. Commun. 192*, 991−998.

Kelly, J. W. (1996) *Curr. Opin. Struct. Biol. 6*, 11−17.

Kelly, J. W., & Lansbury, P. T. J. (1994) *Amyloid 1*, 186−205.

Kirschner, D. A., Abraham, C., & Selkoe, D. J. (1986) *Proc. Natl. Acad. Sci. U.S.A. 83*, 503−507.

Kirschner, D. A., Inouye, H., Duffy, L. K., Sinclair, A., Lind, M., & Selkoe, D. J. (1987) *Proc. Natl. Acad. Sci. U.S.A. 84*, 6953−57.

Klunk, W. E., Pettegrew, J. W., Abraham, D. J. (1989) *J. Histochem. Cytochem. 37*, 1293−1297.

Kocisko, D. A., Come, J. H., Priola, S. A., Cheseboro, B., Raymond, G. J., Lansbury, P. T., & Caughey, B. (1994) *Nature 370*, 471−474.

Kocisko, D. A., Priola, S. A., Raymond, G. J., Chesebro, B., Lansbury, P. T., Jr., & Caughey, B. (1995) *Proc. Natl. Acad. Sci. U.S.A. 9*, 3923−3927.

Lansbury, P. T. (1992) *Biochemistry 31*, 6865−6870.

Lansbury, P. T. (1995) *Chem. Biol. 2*, 1−5.

Lee, J. P., Stimson, E. R., Ghilardi, J. R., Mantyh, P. W., Lu, Y. A., Felix, A. M., Llanoss, W., Behbin, A., Cummins, M., Vancriekinge, M., Timms, W., & Maggio, J. E. (1995) *Biochemistry 34*, 5191−5200.

Makover, A., Moriwaki, H., Ramakrishnan, R., Saraiva, M. J. M., Blaner, W. S., & Goodman, D. S. (1988) *J. Biol. Chem. 263*, 8598−8603.

McCutchen, S., & Kelly, J. W. (1993) *Biochem. Biophys. Res. Commun. 197*, 415−421.

McCutchen, S., Colon, W., & Kelly, J. W. (1993) *Biochemistry 32*, 12119−12127.

McCutchen, S. L., Lai, Z., Miroy, G., Kelly, J. W., & Colon, W. (1995) *Biochemistry 34*, 13527.

Monaco, H. L., Rizzi, M., & Coda, A. (1995) *Science 268*, 1039−1041.

Mulkerrin, M. G., & Wetzel, R. (1989) *Biochemistry 28*, 6556−6561.

Nguyen, J., Baldwin, M. A., Cohen, F. E., & Prusiner, S. B. (1995) *Biochemistry 34*, 4186−4192.

Nilsson, S. F., Rask, L., & Peterson, P. A. (1975) *J. Biol. Chem. 250*, 8554−8563.

Pan, K. M., Baldwin, M., Nguyen, J., Gasset, M., Serban, A., Groth, D., Mehlhorn, I., Huang, Z., Fletterick, R. J., & Cohen, F. E. (1993) *Proc. Natl. Acad. Sci. U.S.A. 90*, 10962−10966.

Pepys, M. B., Hawkins, P. N., Booth, D. R., Vigushin, D. M., Tennent, G. A., Soutar, A. K., Totty, N., Nguyen, O., Blake, C. C. F., Terry, C. J., et al. (1993) *Nature 362*, 553−557.

Pettersson, T., Carlstrom, A., & Jornvall, H. (1987) *Biochemistry 26*, 4572−4583.

Pras, M., Schubert, M., Zucker-Franklin, D., Rimon, A., & Franklin, E. C. (1968) *J. Clin. Invest. 47*, 924−933.

Prusiner, S. B. (1991) *Science 252*, 1515−1522.

Raz, A., & Goodman, D. S. (1969) *J. Biol. Chem. 244*, 3230−3237.

Safar, J., Roller, P. P., Gajdusek, D. C., & Gibbs, C. J., Jr. (1993) *Protein Sci. 2*, 2206−2216.

Safar, J., Roller, P. P., Gajdusek, D. C., & Gibbs, C. J., Jr. (1994) *Biochemistry 33*, 8375−8383.

Saraiva, M. J. M. (1995) *Hum. Mutat. 5*, 191−196.

Saraiva, M. J. M., Costa, P. P., & Goodman, D. S. (1983) *J. Lab. Clin. Med. 102*, 590−603.

Saraiva, M. J. M., Birken, S., Costa, P., & Goodman, D. S. (1984) *J. Clin Inv. 74*, 104−119.

Saraiva, M. J. M., Costa, P. P., & Goodman, D. S. (1988) *Adv. Neurol. 48*, 189−200.

Schmid, F. X. (1989) in *Protein Structure: a practical approach*, pp 251−285, IRL Press, New York.

Simmons, L. K., May, P. C., Tomaaselli, K. J., Rydel, R. E., Fuson, K. S., Brigham, E. F., Wright, S., Lieberburg, I., Becker, G. W., & Brems, D. N. (1994) *Mol. Pharmacol. 45*, 373−379.

Sipe, J. D. (1992) *Annu. Rev. Biochem. 61*, 947−975.

Sipe, J. D. (1994) *Crit. Rev. Clin. Lab. Sci. 31*, 325−354.

Sorgehan, B., Kosmoski, J., & Glabe, C. (1994) *J. Biol. Chem. 269*, 28551−28554.

Steinrauf, L. K., Hamilton, J. A., Braden, B. C., Murrell, J. R., & Benson, M. D. (1993) *J. Biol. Chem. 268*, 2425−2430.

Stone, M. J. (1990) *Blood 75*, 531−545.

Tan, S. Y., Pepys, M. B., & Hawkins, P. N. (1995) *Am. J. Kidney Dis. 26*, 267−285.

Terry, C. J., Damas, A. M., Oliveira, P., Saraiva, M. J., ALves, I. L., Costa, P. P., Matias, P. M., Sakaki, Y., & Blake, C. C. F. (1993) *EMBO J. 12*, 735−741.

Westermark, P., Sletten, K., Johannson, B., & Cornwell, G. G. (1990) *Proc. Natl. Acad. Sci. U.S.A. 87*, 2843−2845.

Wojtczak, A., Luft, J., & Cody, V. (1992) *J. Biol. Chem. 267*, 353−357.

Woody, R. W. (1985) in *Conformations in Biology and Drug Design*, pp 15−114, Academic Press, New York.

Zhang, H., Kaneko, K., Nguyen, J. T., Livshits, T. L., Baldwin, M. A., Cohen, F. E., James, T. L., & Prusiner, S. B. (1995) *J. Mol. Biol. 250*, 514−526.

BI952501G